



Effects of direct heat stress on summer maize and risk assessment

Qi Zhang¹ · Jiahao Han¹ · Xiaoya Yang¹

Received: 4 May 2021 / Accepted: 25 August 2021 / Published online: 1 September 2021
© The Author(s), under exclusive licence to Springer-Verlag GmbH Austria, part of Springer Nature 2021

Abstract

The frequency and severity of extreme heat have increased in many parts of the world under global warming, seriously threatening food security and sustainable development. Disaster risk assessment provides the basis for disaster prevention and mitigation. The objective of this study was to isolate the direct impacts of extreme heat on summer maize and construct a summer maize extreme heat disaster risk assessment model by considering both extreme heat hazard and summer maize vulnerability. The results revealed that the extreme heat occurrence probability peaks at mid-June to early July in the Haihe Plain. Summer maize vegetative stage (stage I) occurs mainly in this period. This result demonstrates that extreme heat hazards are more serious in stage I than in the other two stages. Summer maize is most vulnerable to direct heat stress at the reproductive stage (stage III), but the effects are relatively limited. The final risk distribution showed that the risk value increased as the hazard level rose, especially for stage I, due primarily to the serious extreme heat hazard. The risk value for stage III is second only to stage I. Even though this stage is most vulnerable to extreme heat, the extreme heat hazard is small. The high extreme heat risk values are found in the western region and gradually decreased to the eastern coastal area. These risk assessment results provide significant guidance for mitigation strategies and reducing summer maize extreme heat disaster risk that will result from a hotter climate.

Keywords Hazard assessment · Vulnerability · Direct heat stress · Summer maize

1 Introduction

Maize is a major cereal crop produced worldwide. As maize demand continues to increase for food, feed, and fuel, global production has increased to over 1100 million Mt in 2019 (FAO 2020). Meteorological disasters are the main factors that restrict stable maize production under climate change. Negative association between growing season temperature and maize production has been observed in many of the maize producing areas (Sakurai et al. 2012; Gabaldón-Leal et al. 2016). Extreme heat plays a significant role in this negative relationship (Lobell et al. 2011). Meanwhile, the frequency and severity of extreme heat have increased around the world during the past decades (Orlowsky and

Seneviratne 2012; Horton et al. 2016; Lu et al. 2018). Disaster risk assessment has become a major research priority for managing extreme events in order to reduce the possible impacts of extreme events (IPCC 2012).

The negative association between extreme heat and maize production can mainly be explained by two mechanisms. The first mechanism includes the indirect effects of high temperatures that increase crop water stress. This can result from reductions in the soil water supply due to high transpiration, or because of high temperatures, increasing crop water demand for soil water (Lobell et al. 2013). The other mechanism is direct heat stress effects on maize organs, such as desiccation of pollen and reductions in net photosynthesis under extreme heat conditions (Bolanos and Edmeades 1996; Crafts-Brandner and Salvucci 2002). Although previous studies have confirmed the negative relationship between growing season extreme heat and production, it is still unclear as to how much of the impact is a result of the direct heat stress independent from the indirect water stress effects. It is hard to isolate the effect of direct heat stress from other environmental elements, especially with regard to statistical studies based on field conditions (Schlenker and

✉ Qi Zhang
zhangq861206@126.com

✉ Xiaoya Yang
002438@nuist.edu.cn

¹ College of Applied Meteorology, Nanjing University of Information Science and Technology, Nanjing 210044, China

Roberts 2009; Deryng et al. 2014) where precipitation shortages and extreme heat may occur concurrently during the growing season. Additionally, the frequency of concurrent drought and extreme heat events is increasing under climate change (Wei et al. 2020). It is critical to quantitatively assess the direct impacts of extreme heat in order to accurately project crop yield and to develop and target management strategies under global warming.

Process-based crop growth simulation models provide a major approach for separating the effects of different factors (such as irrigation, soil, nutrients, crop management, and weather conditions) on crop growth and grain yield formation processes (Saseendran et al. 2005; Abedinpour et al. 2012; Liu et al. 2014; Ren et al. 2016). A large number of crop models have been built during the past decades, and crop models named Decision Support System for Agrotechnology Transfer (DSSAT), AquaCrop, Agricultural Production Systems Simulator (APSIM), World Food Studies (WOFOST) model, and Erosion Productivity Impact Calculator (EPIC) are most prominent models around the world (Camargo and Kemanian 2016). The fundamental structural may differ for different crop models. Before being used, models should be calibrated and validated for a certain region by using field experimental data. Many previous studies have proven that APSIM is an effective tool for estimating the potential effects of environmental and management elements on crop production. APSIM has been widely used for maize in the North China Plain and Northeast China (Liu et al. 2012; Chauhan et al. 2013; Liu et al. 2014; Ren et al. 2016; Sun et al. 2016). Liu et al. (2014) used APSIM to isolate the effects of changes in sowing dates and temperature on maize growth and yield. They demonstrated that although warming climate had a negative impact on maize, adaptation activities such as earlier sowing dates mitigated the negative impacts. Sun et al. (2016) observed that APSIM was able to quantify the positive effect that sunshine hours and the diurnal temperature range at the grain filling stage had on maize yield. Therefore, we selected APSIM to separate the direct impact of extreme heat on maize yield from the effects of other environment or management elements.

Extreme heat researches have mostly focused on the spatial–temporal distribution of extreme heat events and changes in extreme heat event characteristics (Horton et al. 2016; Yang et al. 2017), the relationship between extreme heat and crop growth (Schlenker and Roberts 2009; Lobell et al., 2011, 2013; Deryng et al. 2014), and public health (Johnson and Wilson 2009; Schwarz et al. 2020). Disaster risk assessment studies can estimate the likelihood of hazardous events and potential losses. Disaster risk assessment is necessary for the mitigation of and preparedness for natural disasters (Zhang 2004; Jia et al. 2012). There are several formulas used for disaster risk assessment, and the formula “risk = hazard × vulnerability” advised by the United Nations

International Strategy for Disaster Reduction (UN/ISDR 2007) has been most commonly used in recent years (Shahid and Behrawan 2008; Jia et al. 2012; Zhang et al. 2017, 2019). Hazard is expressed by the frequency and severity of hazardous events with potentially large impacts (IPCC 2007). For extreme heat hazard, cumulation of degree days over the extreme heat threshold or the number of extreme heat days at crop growing season is mostly used as the severity of extreme heat (Deryng et al. 2014; Zhang et al. 2021). The vulnerability of a hazard-bearing body is the propensity or predisposition to be adversely affected (Zhang et al. 2019). There are several approaches to assess vulnerability, and the method of vulnerability curves has been used by a lot of researchers (Jia et al. 2012; Wang et al. 2013; Yin et al. 2014; Zhang et al. 2019). The curve is expressed as the function between potential losses change with intensities of hazardous events, and logistical function was most commonly used to fit the vulnerability curve in previous studies (Jia et al. 2012; Wang et al. 2013; Yin et al. 2014). Crop models can be used to estimate the potential losses under various environment conditions.

It is difficult to isolate the impacts of direct heat stress on crops, and previous agrometeorological disaster risk assessment research has seldom been concerned about extreme heat, especially the direct stress. In this study, we used summer maize as the hazard-bearing body to assess the risk of direct extreme heat stress by considering two aspects: hazard and vulnerability. Extreme temperature days during each maize growing stage were used to assess the hazard. The calibrated APSIM model was used to separate the direct impacts of extreme heat from other environment factors. Extreme heat vulnerability curves for several summer maize growing stages were constructed. Risk evaluation based on hazard and crop vulnerability can provide the theoretical and scientific bases for extreme heat risk reduction, mitigation, and management strategies.

2 Materials and methods

2.1 Study area

The Haihe Plain (34.93° N–41.06° N; 112.56° E–119.85° E) is the northern part of the North China Plain (Fig. 1). This region produces about 8.5% of China’s total maize output and accounts for 9.9% of China’s maize planting area (Xue et al. 2021). The cropping system is winter wheat and summer maize rotation. It is an area of China where maximum temperatures have been observed in the last few decades (Kang and Eltahir 2018). Compared with southern parts of the North China Plain, the Haihe Plain is with less precipitation and irrigation is required to supplement soil water to achieve much more crop yield (Wu et al. 2019).

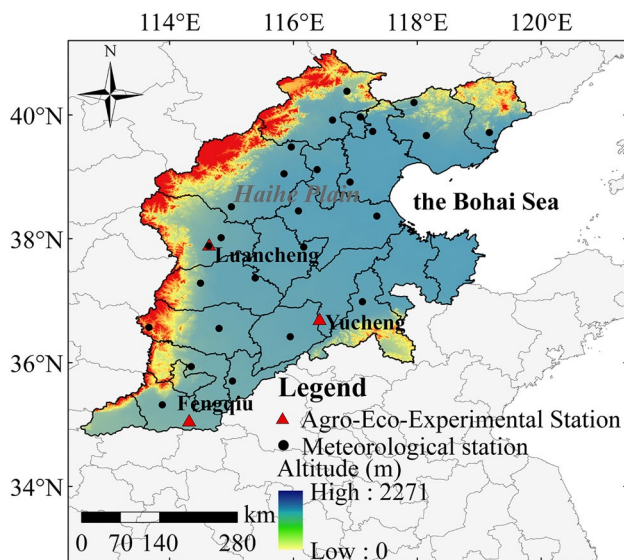


Fig. 1 Study area and meteorological and Agro-Eco-Experimental stations in the Haihe Plain, China

Consequently, the region suffers from some ecological and environmental problems, and irrigation may have aggravated the local extreme heat in recent years (Kang and Eltahir 2018).

2.2 Weather and phenological phase data

Daily maximum temperature, minimum temperature, precipitation, and sunshine duration of 26 meteorological stations at the Haihe Plain were used in this study (Fig. 1); the time range from 1981 to 2019. These weather data are maintained by the China Meteorological Administration and can be accessed at <http://data.cma.cn/>. Rigorous quality control procedures have been performed for the dataset by the maintainers, and it is one of the best daily meteorological datasets in China (Chen and Li 2017). Sunshine duration can be converted into solar radiation using the Ångström formula (Ångström 1924). These daily weather data were used to identify extreme heat and to drive APSIM.

The summer maize yearly phenological stage data included planting, six leaves fully emerged (V6), tasseling (VT), and physiological maturity (R6) dates (stage designations are as given by Ritchie et al. 1986). These phenological dates were collected from the annual report of national agricultural meteorological observation stations, and the paper report forms are maintained by the China Meteorological Administration. These phenological stage dates were used to define three maize growing stages. Stage I: planting to V6 is the vegetative stage, lasting about 34 days; stage II: V6 to VT is the vegetative transitioning to reproductive stage, lasting about 20 days; and stage III: VT to R6 is the reproductive stage, lasting about 45 days. Because cropping calendars and

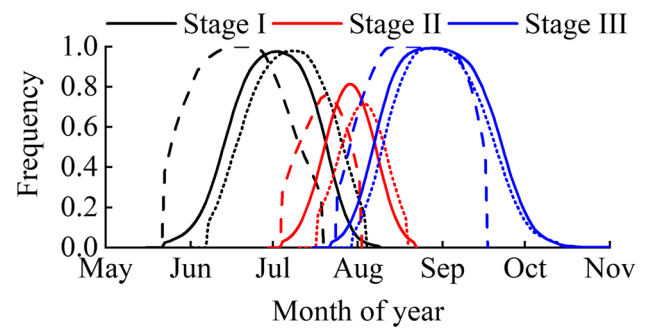


Fig. 2 Frequency of years with summer maize in a certain growing stage on each given date. Black lines show growing stage I, red lines show stage II, and blue lines show stage III. Dashed lines are for the station with the earliest planting dates (Tangyin station), the dotted lines are for the station with the latest planting dates (Huanghua station), and the solid lines show the mean developmental stage distribution averaged across all stations

seasonal temperatures can be different, the growing stages covered different time ranges in different years at different stations. This means that on the same day in different years, summer maize can be in different growing stages. Figure 2 shows that on any given date, the frequency represents the percentage of years that summer maize was within a particular growing stage on a given date. The station with the earliest planting dates is shown as the dashed lines, where planting occurred in late May or early June for most years. The station with the latest planting dates is shown as the dotted lines, where planting occurred in late June for most years (about a month later than the station with the earliest planting dates). The solid lines are the average of all of the stations in the Haihe Plain, where most stations were planted in middle June, V6 occurred in the middle of July, and VT occurred in early August. Variations in cropping calendars and seasonal temperatures result in substantial changes in the temperatures that summer maize may experience, so it is important to use the specific summer maize phenological stage dates.

2.3 Experimental data

Field experiments were conducted at three Agro-Eco-Experimental Stations of the Chinese Academy of Sciences during 2004–2007 (Fig. 1), named Luancheng (LC), Yucheng (YC), and Fengqiu (FQ). All experimental data are supported by the Chinese Ecosystem Research Network (CERN). The multi-year average annual rainfall (AR), annual daily temperature (ADT), and total sunshine hours per year (TSH) are shown in Table 1. All stations belong to the warm temperate semi-humid monsoon climate, with rainfall mainly concentrated in summer. The soil is classified as loamy soil at LC and YC and sandy loam at FQ. The bulk density and hydraulic parameters in various soil layers at the

Table 1 Climatic conditions at three Agro-Eco-Experimental Stations in the Haihe Plain, China, including annual daily temperature (ADT), total sunshine hours (TSH), and annual rainfall (AR)

Sites	Location	Altitudes (m)	ADT (°C)	TSH (h)	AR (mm)
LC	37°53 N, 114°40 E	50.1	12.3	2608	481
YC	36°40 N, 116°22 E	20.0	13.3	2640	515
FQ	35°01 N, 114°20 E	67.5	13.9	2310	605

Note: LC, YC, and FQ are the abbreviations of Luancheng, Yucheng, and Fengqiu station, respectively

experimental stations are shown in Table 2. These data are local experimental station data sets and from CERN.

The field experimental data were used to calibrate APSIM. Experimental data at LC were recorded during 2005–2007 for maize variety “Jingyu 7.” Fertilizer was applied at V6 as 90 kg N ha⁻¹, 90 kg ha⁻¹ P₂O₅, and 45 kg ha⁻¹ K₂O. Experimental data at YC were recorded during 2005–2007 for maize variety “Ludan 9002.” Fertilizer was applied at V6 as 150 kg N ha⁻¹, 75 kg ha⁻¹ P₂O₅, and 75 kg ha⁻¹ K₂O. Experimental data at FQ were recorded during 2004–2007 for maize variety “Zhengdan 958.” Fertilizer was applied before planting as 90 kg N ha⁻¹, 90 kg ha⁻¹ P₂O₅, and 90 kg ha⁻¹ K₂O. Experimental data are all from non-water-stress experiments. Irrigation was applied when soil water content was low and the irrigation method was flooding. Phenological development, biomass, leaf-area

index (LAI), and grain yield were observed at each growing season and were used to calibrate APSIM.

2.4 APSIM model and calibration

APSIM was developed by the Agricultural Production Systems Research Group (APSRU) under the Commonwealth Scientific and Industrial Organization of Australia (CSIRO) and the Queensland Government. The APSIM maize model has been well validated and can be downloaded from the APSIM website (<https://www.apsim.info/>). APSIM version 7.10 was used in this study to separate the direct impacts of extreme heat on maize yields from other climate or management elements and then to build the summer maize extreme heat vulnerability curves at different growing stages.

APSIM was calibrated by comparing simulated results with experimentally observed data that included above-ground biomass, leaf-area index (LAI), and grain yield at LC, YC, and FQ with a trial-and-error method (Seidel et al. 2018). The coefficients of determination (R^2), slopes of regression lines, and root mean squared errors (RMSE) were used to quantify model performance.

2.5 APSIM model-based risk assessment process

2.5.1 Hazard assessment

The number of extreme heat days was used as the hazard intensity factor (H). For summer maize, daily maximum temperature over 35 °C can be considered an extreme heat

Table 2 Soil characteristics in different soil layers at three experimental stations in the Haihe Plain, China, including soil bulk density (BD), volumetric water content at saturation (SAT), drained upper limit (DUL), and lower limit of plant available soil water (LL)

Sites	Soil depth (cm)	BD (g/m ³)	SAT (mm/mm)	DUL (mm/mm)	LL (mm/mm)
LC	0–10	1.423	0.44	0.36	0.10
	10–20	1.611	0.46	0.35	0.11
	20–40	1.558	0.46	0.35	0.11
	40–60	1.429	0.43	0.33	0.14
	60–100	1.433	0.44	0.34	0.14
	100–150	1.433	0.44	0.34	0.14
YC	0–10	1.342	0.40	0.32	0.06
	10–20	1.415	0.41	0.31	0.07
	20–40	1.419	0.41	0.34	0.08
	40–60	1.452	0.42	0.33	0.10
	60–100	1.510	0.42	0.30	0.11
	100–150	1.510	0.43	0.28	0.10
FQ	0–10	1.409	0.43	0.21	0.12
	10–20	1.536	0.43	0.21	0.12
	20–40	1.536	0.41	0.32	0.13
	40–60	1.368	0.41	0.32	0.12
	60–100	1.407	0.44	0.32	0.12
	100–150	1.407	0.44	0.36	0.12

Note: LC, YC, and FQ are the abbreviations of Luancheng, Yucheng, and Fengqiu station, respectively.

day (Deryng et al. 2014). Because the sensitivities of summer maize to extreme heat vary at different growing stages, the hazard intensities were calculated for each stage separately. Based on the concept of hazard, a hazard assessment model was constructed from the perspectives of the probability and intensity (Zhang et al. 2017, 2019).

$$H = \sum_{s=1}^n S \times f(S) \tag{1}$$

where H is the hazard assessment value for a certain station, S is the number of observed extreme heat days during a summer maize growing stage (denoting the intensity of extreme heat), and $f(S)$ is the frequency of years with S days of extreme heat during this growing stage.

2.5.2 Vulnerability curves

In this study, we simulated two scenarios: standardized climate scenario with no heat stress (S1) and temperature change scenario (S2). Summer maize yields under the two scenarios were simulated by the calibrated APSIM model. S1 was conducted to simulate the yield under standardized climate conditions by driving the APISM model with multi-year average daily temperature, precipitation, and solar radiation data. S2 was conducted to examine the influence of changes in temperatures during a certain growing stage on final crop yield. We did this by driving the APSIM model with actual temperature data during a certain growing stage during the past 40 years, while the temperature data used during the other growing stages, as well as precipitation and solar radiation, were multi-year average daily data. For both of the scenarios, we simulated no water and nutrient stresses by setting automatic irrigation and fertilization in APSIM. Under such conditions, the simulated yield variations (YL) between S2 and S1 can denote the direct effects of temperature at the studied growing stage, excluding other elements, such as the water stress. The vulnerability curve of each growing stage was obtained by establishing the function between YLs and extreme heat hazard intensities (H). In this study, logistical functions were used to fit the vulnerability curves. YL values were calculated as

$$YL_{ij} = \frac{Yield_1 - Yield_{2ij}}{Yield_1} \tag{2}$$

where YL_{ij} is the yield variations at growing stage i and year j . $Yield_1$ is yield under S1. $Yield_{2ij}$ is the yield under S2 for growing stage i and year j .

2.5.3 Calculation of disaster risk

According to regional disaster system theory, disaster risk (R) is a function of hazard (H) and vulnerability (V) under

the influence of environment. Equation (4) was used to express risk in this study (Shi 2002; UN/ISDR 2007; Yin et al. 2014; Zhang et al. 2017; Zhang et al. 2019).

$$R = f(H, V) = YL_H, V\{YL, H\} \tag{3}$$

where YL_H is the yield losses resulted by the direct impact of extreme heat; H_i is the extreme heat hazard intensity with i -year return period, the return period is calculated by the exceeding probability of extreme heat intensity at each station; $V\{YL, H\}$ is the function for YL versus H (the vulnerability curve); YL_{H_i} can be calculated according to $V\{YL, H\}$. The overall technological framework of risk assessment is described in Fig. 3.

3 Results

3.1 Performance of APSIM model

Comparisons of simulated maize LAI, aboveground biomass, and yield with measured values are shown in Fig. 4. The variations in observed LAI, aboveground biomass, and grain yield in different years and experimental stations are well captured by APSIM. Slope values (β) are near to 1.0, indicating that there are no obvious systematic over- or under-estimations. The R^2 values indicate that the model-simulated values explained 97%, 98%, and 81% of

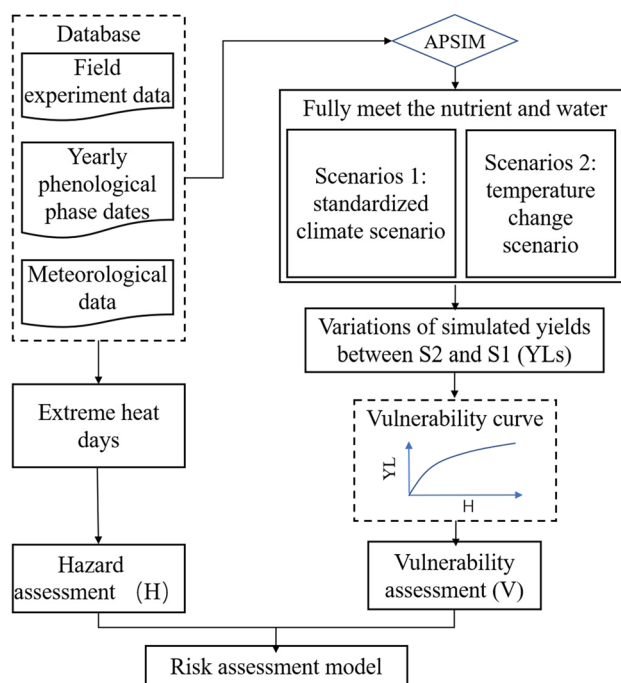


Fig. 3 Risk assessment process for direct extreme heat stress on summer maize

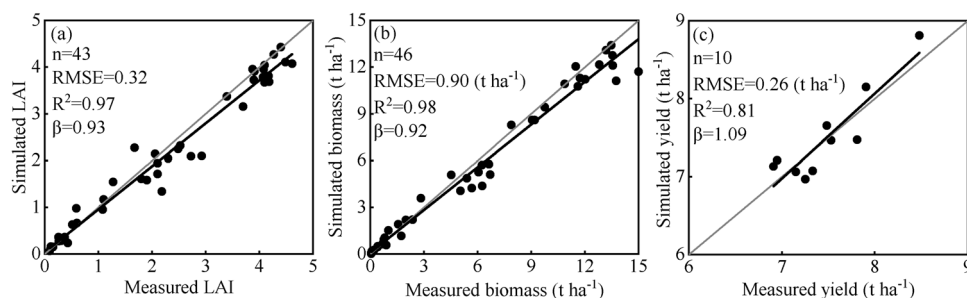


Fig. 4 Comparisons between observed and simulated LAI, biomass, and grain yield from 2004 to 2007 at Luancheng, Yucheng, and Fengqiu. n =number of observations; R^2 =coefficient of determination;

β =regression slope; RMSE=root mean square error. The gray lines are the 1:1 lines; the black lines are the linear regression lines

the variation in measured LAI, biomass, and grain yield, respectively.

3.2 Extreme heat hazard assessment

During 1981–2019, the earliest date of extreme heat in the Haihe Plain appeared on April 17, 2019 at Shexian, and the latest date of extreme heat was on September 19. As shown in Fig. 5a, the frequencies of the occurrence of extreme heat days were highest from mid-June to early July, and the frequencies were mostly greater than 0.2. The frequency decreased as the day sequence increased, but a small spike appeared around July 23. Luancheng had the largest number of extreme heat days of all the stations (16.7 day per year). Changli had the least number of extreme heat days (2.5 day per year).

Based on the summer maize yearly phenological stage dates at each station, we extract the number of extreme heat days at each growing stage, and the annual variations are shown in Fig. 5b. The year 1997 was very hot, and the average number of extreme heat days during summer maize growing season in the Haihe Plain reached 21.4 days (black solid line). Before 1997, the multi-year average number of

extreme heat days was 7.0 days (gray dashed line). Since 1997, the number of extreme heat days increased to an average of 11.1 days. The multi-year average ratio of extreme heat days during the entire growing season to that during the year was 77.6%. The red, blue, and green solid lines in Fig. 5b show the annual variation of the number of extreme heat days during summer maize growing stages I–III, respectively. The percentage of the entire growing season with extreme heat days during the three growing stages were 74.0%, 19.0%, and 7.0%, respectively. This means that in the Haihe Plain, extreme heat mainly occurred during the summer maize growing season, especially during stage I (planting to V6).

Based on Eq. (1), extreme heat hazard values during each growing stage at each station are calculated, and the spatial distributions are shown in Fig. 6. The spatial distributions are consistent for the growing season and for growing stages I and II. The extreme heat hazards are the smallest at the northeastern coastal area for all stages and increased to the western area. For stage III, the extreme heat hazard for the entire region is very low. The spatial variation is larger at stage I, with a range of 9.7 days, while at stage II the range is only 3.8 days.

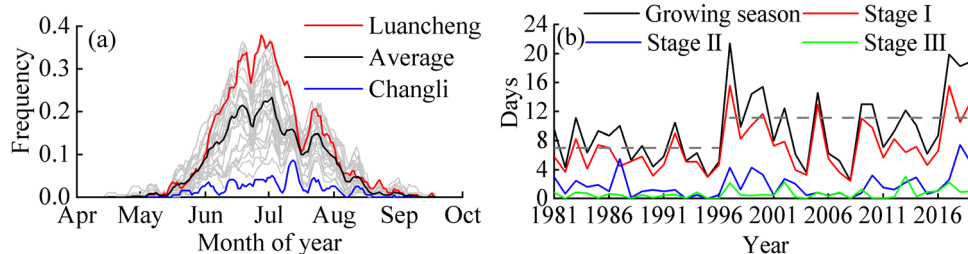
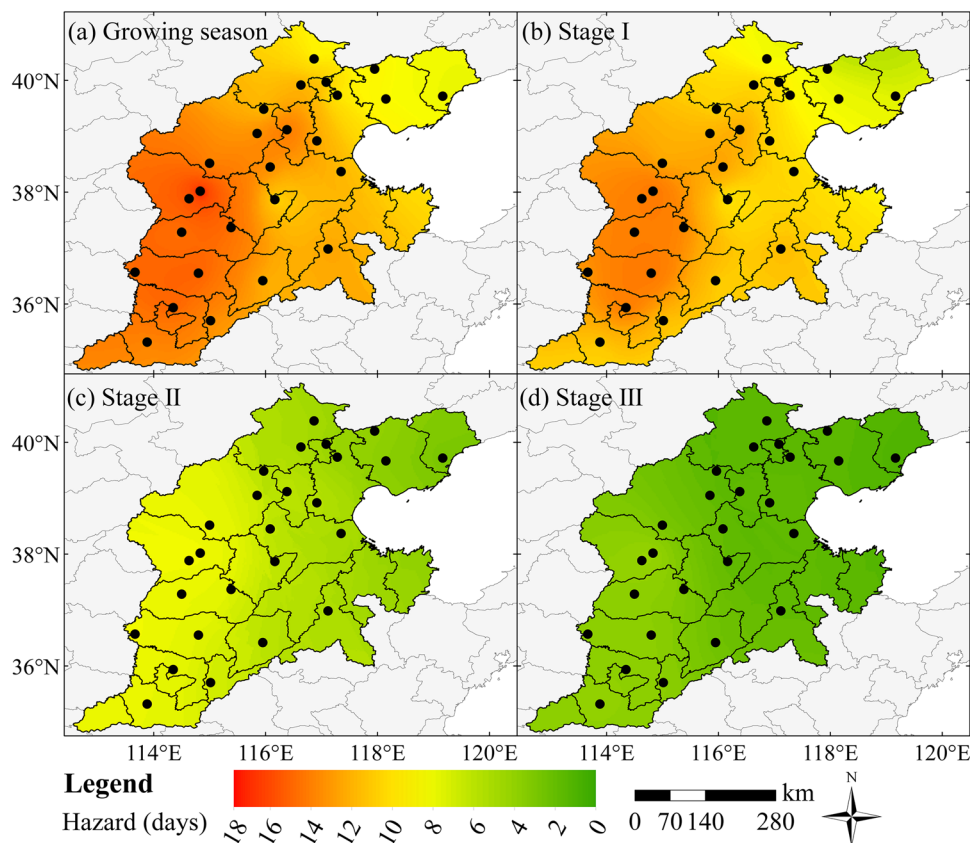


Fig. 5 Distribution of extreme heat days in the Haihe Plain, China. **a** Frequency of extreme heat for a certain day during the past 39 years. The lines are the 5-day moving average frequency at different stations. The red solid line denotes Luancheng, the location with the most frequent extreme heat; the solid blue line denotes Changli, the location with the smallest number of extreme heat days; the solid black line is the average of all of the stations in the Haihe Plain;

the gray lines are other stations. **b** Annual variation of the number of extreme heat days at each summer maize growing stage. The solid black line denotes the entire growing season; the solid red line denotes stage I; the solid blue line denotes stage II; the solid green line denotes stage III; the gray dashed lines are the multi-year average number of extreme heat days during the entire growing season before and since 1997

Fig. 6 Summer maize extreme heat hazard distribution. **a** Entire growing season; **b** stage I; **c** stage II; **d** stage III



3.3 Extreme heat vulnerability at each summer maize growing stage

Based on the calibrated APSIM model and the process introduced in Sect. 2.5, maize yields are simulated under different numbers of extreme heat days at each summer maize growing stage. Logistical functions are used to fit the yield losses against extreme heat intensity at each growing stage. The final vulnerability curves are shown in Fig. 7, and the function parameters and R^2 values are shown in Table 3. The fitting goodness of vulnerability curve for stage I is the best, and its R^2 is 0.44. The fitted curves of the three stages all at the 0.01 significance level explained most of the variability. By comparing the vulnerability curves of the three growing stages, it can be seen that summer maize is more vulnerable to extreme heat direct stress at stage III. At this stage, the number of extreme heat days over 1.6 days could result in yield losses, and yield losses increased rapidly with the number of extreme heat days. At stage I, the extreme heat days over 9.1 days may result in yield losses, and yield losses increased slowly with the number of extreme heat days. Stage I is the least sensitive stage among the three growing stages. Vulnerability of stage II is intermediate to stage I and stage 3, and the number of extreme heat days over 4.4 days could result in yield losses at this stage. In general, the yield losses resulting from direct heat stress are

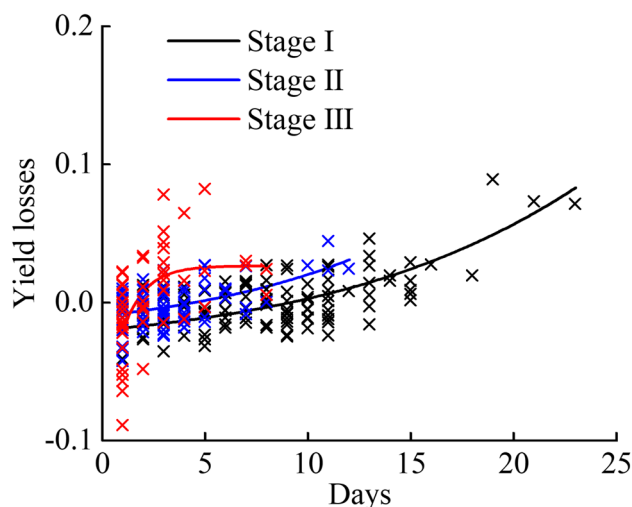


Fig. 7 Physical vulnerability curves for direct heat stress on summer maize at different growing stages. The yield loss and the extreme heat intensity of a site in a given year are indicated by a cross, black crosses represent growing stage I, blue crosses represent growing stage II, red crosses represent growing stage III. The curves are fitted by using logistical function called vulnerability curves

limited, as shown in Fig. 7. APSIM simulated yield losses of less than 10% under historical temperature conditions and with water demand fully met by irrigation (no water stress).

Table 3 Functions of vulnerability curves for summer maize different growing stages

Stage	Function of vulnerability curves	R^2
Stage I	$y = \frac{1}{1+64.5435e^{-0.0939x}} - 0.0352$	0.44
Stage II	$y = \frac{1}{1+62.8441e^{-0.1101x}} - 0.0253$	0.30
Stage III	$y = \frac{1}{1+0.1274e^{-0.9583x}} - 0.9736$	0.36

3.4 Risk assessment of direct extreme heat stress on summer maize

Risk of the direct extreme heat stress is assessed based on the vulnerability curves and extreme heat hazard. Annual extreme heat intensity for each summer maize growing stage at every station is recognized, and the exceeding probability of extreme heat intensity for each station is fitted. With the corresponding vulnerability curves, 5-year, 10-year, 20-year, and 50-year return period summer maize extreme heat risk maps are drawn (Fig. 8). As the return period increases, the risk values increase gradually, and the increased amplitude is quite large for stage I, especially in the western area. As shown in Fig. 6, growing stage I has the greatest extreme heat hazard, especially in the western region. Although summer maize is not very vulnerable to extreme heat direct stress at this stage, the extremely large numbers of extreme heat days make the risk values large. For stages II and III, extreme heat hazards are less, but stage III is the most vulnerable period to extreme heat direct stress, thereby making the risk values larger for stage III at the same hazard level.

4 Discussion and conclusions

4.1 Discussion

Extreme heat and drought are often concurrent. Extreme heat can result in yield losses by increasing water stress or by direct heat stress effects. It is critical to analyze the direct temperature impacts for accurate yield prediction and targeted mitigation strategies (Carter et al. 2016). In our research, APSIM was used to separate the direct impacts of extreme heat from other parameters, including impacts associated with soil water stress, as we set APSIM to simulate with water requirement fully met. There is no doubt that extreme heat would reduce maize yield. Our results further quantify the direct impacts of extreme heat on summer maize yield during different growing stages. The number of these instances are relatively limited but cannot be alleviated by irrigation (Fig. 7). This is in agreement with earlier studies in the central USA (Lobell et al. 2013; Zhang et al. 2015) that reported that extreme heat effects resulted by reducing soil water supply played a greater role

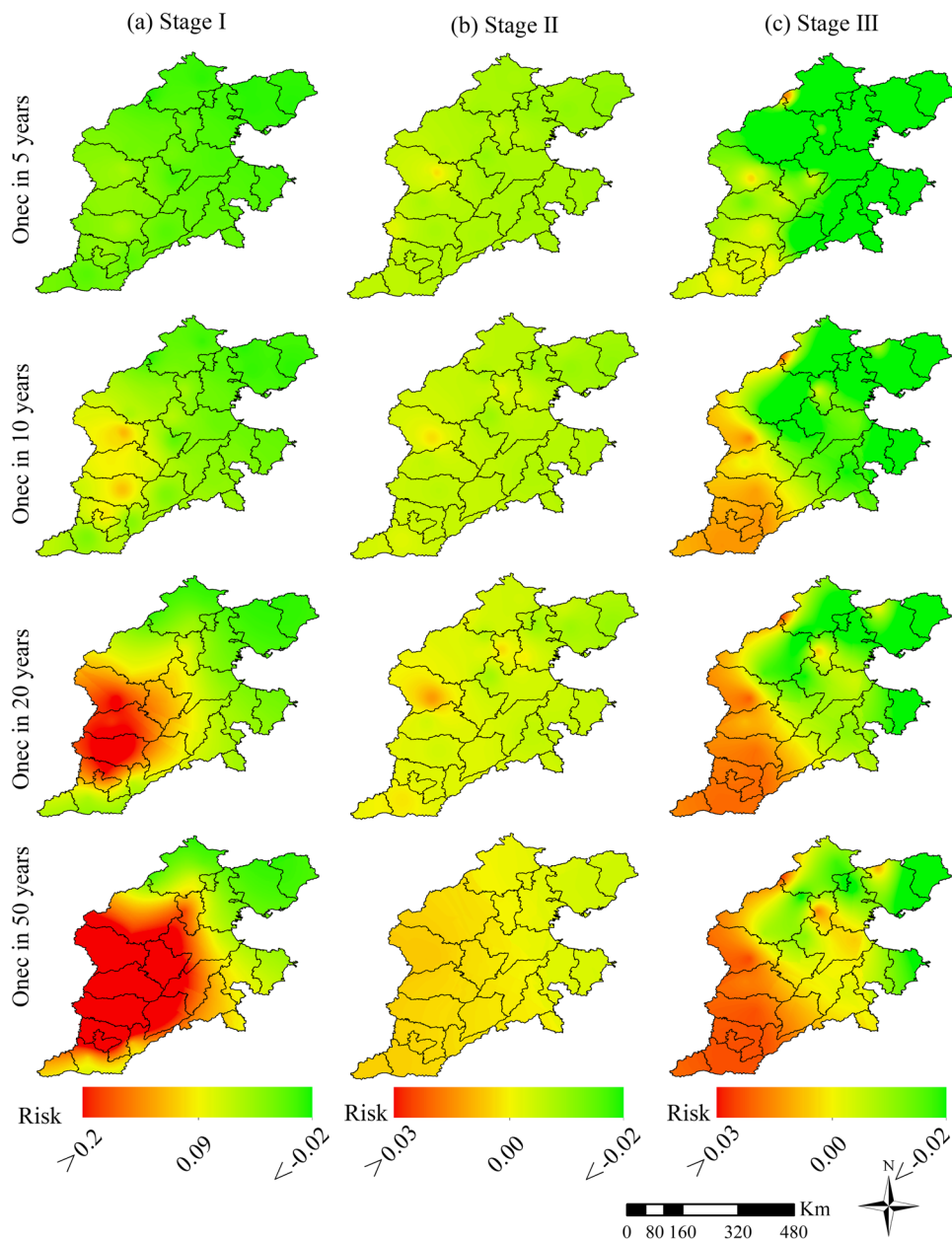
in yield reductions and irrigation can significantly reduce the sensitivity of maize to extreme heat. Over two-thirds of the negative effects can be reduced by irrigation. The area equipped for irrigation is large in the Haihe Plain (Kang and Eltahir 2018), and irrigation has relieved the impacts of extreme heat and insufficient precipitation. However, the large amount of irrigation water requirement has led to a declining groundwater table in this region and has exacerbated water shortages and environmental issues (van Oort et al. 2016). Risk adaptation strategies, such as breeding cultivars to ameliorate heat damage or shifting current cropping systems to use of heat tolerant crops, are necessary. Carter et al. (2016) assumed that improved genetics and management strategies have the potential to partially or completely eliminate the impacts of extreme heat on maize.

When studying extreme hazards during the different summer maize growing stages, some researchers have used fixed phenological dates, such as the average dates across years, or they have presumed the phenological dates are the same across regions (Jia et al. 2012; Zhang et al. 2017). These assumptions cannot represent year-to-year variations or differences between regions. Correctly resolving growing stages is quite important in considering yield sensitivity (Butler and Huybers 2015). In our study, specific summer maize stage dates were used to quantify extreme heat intensity and vulnerability curves for each growing stage. This method permits better understanding of extreme heat and crop growth and provides a more accurate risk assessment result for better guidance of heat stress mitigation strategies and yield prediction.

Many previous studies have confirmed that silking and grain filling are the maize stages most sensitive to extreme heat (Sánchez et al. 2014; Butler and Huybers 2015). Our results, as shown in Fig. 7, are consistent with these previous studies. Additionally, our results further determined that the extreme heat disaster risks are different at different growing stages. Even though growing stage III has the greatest vulnerability to direct extreme heat stress, the extreme heat hazards are relatively small, and the final disaster risks are not serious (Fig. 8). An effective method for reducing summer maize extreme heat disaster risk could be to adjust planting dates so that the highly temperature-sensitive stage does not occur during the time of year when high temperatures frequently occur.

Summer maize extreme heat vulnerability curves have the potential to predict yield losses according to the growing season extreme heat condition; this is quite valuable for extreme heat disaster early warning, risk management, agricultural insurance, etc. However, the fitting goodness of the vulnerability curve presented in this study still has the space to be further promoted. Moreover, it is built based on crop model. Crop model simulation results are related with the model calibration strategies; this may lead to some errors

Fig. 8 Risk of direct extreme heat stress on summer maize at different growing stages in the Haihe Plain, China, with hazard levels of once in 5, 10, 20, and 50 years



in regional scale application. Vulnerability curves built by the detailed and high-quality historical disaster records are closest to the production practice; however, such records are lacking in many areas. The more realistic vulnerability curve can greatly improve the accuracy of summer maize yield forecasting and disaster early warning, which should be further explored in future researches.

4.2 Conclusions

The present study assessed the risk of direct extreme heat stress on summer maize in Haihe Plain based on the regional disaster risk system theory. Hazard and vulnerability are considered in the risk assessment model. The major

conclusions are as follows: (1) In Haihe Plain, extreme heat days most commonly occur in mid-June to early July. For most years and stations, this period coincides with summer maize growing stage I. This results in an extreme heat hazard at this stage that is significantly larger than observed for growing stages II and III. And the hazards appeared higher in the western part of the study area. (2) The fitted vulnerability curves for the three growing stages showed that summer maize is most vulnerable to direct heat stress at growing stage III, followed by stages II and I. However, yield losses that are a result of direct heat stress are relatively limited. (3) Summer maize extreme heat disaster risk increased as hazard levels rose, and the increased magnitude is larger in growing stage I, especially for the western area.

This result is mainly due to serious extreme heat hazard. Growing stage III followed due to high vulnerability. The risk assessment results are significant because they provide the basis for a better understanding of how to reduce summer maize extreme heat disaster risk that may arise from a hotter future climate.

Author contribution All authors contributed to the study conception and design. Data collection and analysis were performed by Jiahao Han and Qi Zhang. The first draft of the manuscript was written by Qi Zhang and Xiaoya Yang. All authors read and approved the final manuscript.

Funding This work was jointly supported by the National Key Research and Development Program of China under Grant No. 2019YFC1510205 and National Natural Science Foundation of China under Grant No. 41977410.

Availability of data and material The weather data that support the findings of this study are available from the China Meteorological Administration and can be accessed at "<http://data.cma.cn/>." The summer maize phenological phase data and experimental data that support the findings of this study are not openly available due to reason of sensitivity and are available from the corresponding author on reasonable request.

Code availability Not applicable.

Declarations

Ethics approval Not applicable.

Consent to participate Not applicable.

Consent for publication Not applicable.

Conflict of interest The authors declare no competing interests.

References

- Abedinpour M, Sarangi A, Rajput TBS, Singh M, Pathak H, Ahmad T (2012) Performance evaluation of AquaCrop model for maize crop in a semi-arid environment. *Agric Water Manag* 110:55–66
- Ångström A (1924) Solar and terrestrial radiation. *J Quart J Roy Met Soc* 50:121–125
- Bolanos J, Edmeades GO (1996) The importance of the anthesis-silking interval in breeding for drought tolerance in tropical maize. *Field Crops Res* 48:65–80
- Butler EE, Huybers P (2015) Variations in the sensitivity of US maize yield to extreme temperatures by region and growth phase. *Environ Res Lett* 10(3):034009
- Camargo GGT, Kemanian AR (2016) Six crop models differ in their simulation of water uptake. *Agric for Meteorol* 220:116–129
- Carter EK, Melkonian J, Riha SJ, Shaw SB (2016) Separating heat stress from moisture stress: analyzing yield response to high temperature in irrigated maize. *Environ Res Lett* 11(9):094012
- Chauhan YS, Solomon KF, Rodriguez D (2013) Characterization of north-eastern Australian environments using APSIM for increasing rainfed maize production. *Field Crops Res* 144:245–255
- Chen Y, Li Y (2017) An inter-comparison of three heat wave types in China during 1961–2010: observed basic features and linear trends. *Sci Rep* 7:45619
- Crafts-Brandner SJ, Salvucci ME (2002) Sensitivity of photosynthesis in a C4 plant, maize, to heat stress. *Plant Physiol* 129:1773–1780
- Deryng D, Conway D, Ramankutty N et al (2014) Global crop yield response to extreme heat stress under multiple climate change futures. *Environ Res Lett* 9(3):034011
- FAO Food and Agriculture Organization of the United Nations (FAO) (2020) FAO Statistical Databases, Accessed December 2020 available at <http://faostat.fao.org>
- Gabaldón-Leal C, Webber H, Otegui ME, Slafer GA, Ordóñez RA, Gaiser T, Lorite IJ, Ruiz-Ramos M, Ewert F (2016) Modelling the impact of heat stress on maize yield formation. *Field Crops Res* 198:226–237
- Godwin DC, Ritchie JT, Singh U, Hunt L (1989) A user's guide to CERES-Wheat v2.1 International Fertilizer Development Centre. Muscle Shoals, AL
- Horton RM, Mankin JS, Lesk C, Coffel E, Raymond C (2016) A review of recent advances in research on extreme heat events. *Current Climate Change Reports* 2(4):242–259
- IPCC (2007) Climate Change 2007: Impacts, adaptation and vulnerability contribution of Working Group 2 to the Fourth Assessment Report of the Intergovernmental Panel on Climate Change. Cambridge University Press, Cambridge
- IPCC (Intergovernmental Panel on Climate Change) (2012) Managing the risks of extreme events and disasters to advance climate change adaptation: special report of the Intergovernmental Panel on Climate Change. Cambridge University Press, New York
- Jia H, Wang J, Cao C, Pan D, Shi P (2012) Maize drought disaster risk assessment of China based on EPIC model. *International Journal of Digital Earth* 5(6):488–515
- Johnson DP, and Wilson JS (2009) The socio-spatial dynamics of extreme urban heat events: the case of heat-related deaths in Philadelphia. *Appl Geog* 29(3):419–434
- Kang S, Eltahir EAB (2018) North China Plain threatened by deadly heatwaves due to climate change and irrigation. *Nat Commun* 9:2894
- Liu Z, Yang X, Hubbard KG, Lin XM (2012) Maize potential yields and yield gaps in the changing climate of northeast China. *Glob Chang Biol* 18(11):3441–3454
- Liu Z, Hubbard KG, Lin X, Yang X (2014) Negative effects of climate warming on maize yield are reversed by the changing of sowing date and cultivar selection in Northeast China. *Glob Chang Biol* 19(11):3481–3492
- Lobell DB, Hammer GL, McLean G, Messina C, Roberts MJ, Schlenker W (2013) The critical role of extreme heat for maize production in the United States. *Nat Clim Chang* 3(5):497–501
- Lobell DB, Banziger M, Magorokosho C, Vivek B (2011) Nonlinear heat effects on African maize as evidenced by historical yield trials. *Nature Clim Change* 1:42–45
- Lu Y, Hu H, Li C, Tian F (2018) Increasing compound events of extreme hot and dry days during growing seasons of wheat and maize in China. *Sci Rep* 8(1):16700
- Orlowsky B, Seneviratne SI (2012) Global changes in extreme events: regional and seasonal dimension. *Clim Change* 110(3–4):669–696
- Ren X, Sun D, Wang Q (2016) Modeling the effects of plant density on maize productivity and water balance in the Loess Plateau of China. *Agric Water Manag* 171:40–48
- Ritchie SW, Hanway JJ, Benson GO (1986) How a corn plant develops. Spec. Rep. No. 48. Iowa State Univ. Coop. Ext. Serv., Ames, IA

- Sakurai G, Iizumi T, Yokozawa M (2012) Varying temporal and spatial effects of climate on maize and soybean affect yield prediction. *Clim Res* 49:143–154
- Saseendran SA, Ma L, Nielsen DC, Vigil MF, Ahuja LR (2005) Simulating planting date effects on corn production using RZWQM and CERES-maize models. *Agron J* 97(1):58–71
- Sánchez B, Rasmussen A, Porter JR (2014) Temperatures and the growth and development of maize and rice: a review. *Glob Change Biol* 20(2):408–417
- Schlenker W, Roberts MJ (2009) Nonlinear temperature effects indicate severe damages to US crop yields under climate change. *Proc Natl Acad Sci* 106(37):15594–15598
- Schwarz L, Malig B, Guzman-Morales J et al (2020) The health burden fall, winter and spring extreme heat events in the in Southern California and contribution of Santa Ana Winds. *Environ Res Lett* 15(5):054017
- Seidel SJ, Palosuo T, Thorburn P, Wallach D (2018) Towards improved calibration of crop models – Where are we now and where should we go? *Eur J Agron* 94:25–35
- Shahid S, Behrawan H (2008) Drought Risk Assessment in the Western Part of Bangladesh 46(3):391–413
- Shi PJ (2002) Theory on disaster science and disaster dynamics. *Journal of Natural Disasters* 11(3):2–10 ((In Chinese))
- Sun H, Zhang X, Wang E, Chen S, Shao L, Qin W (2016) Assessing the contribution of weather and management to the annual yield variation of summer maize using APSIM in the North China Plain. *Field Crop Res* 194:94–102
- UN/ISDR (United Nations International Strategy for Disaster Reduction) (2007). *Living with risk. A global review of disaster reduction initiatives*. Geneva: UN/ISDR
- van Oort PAJ, Wang G, Vos J (2016) Towards groundwater neutral cropping systems in the Alluvial Fans of the North China Plain. *Agric Water Manag* 165:131–140
- Wang L, Liao S, Huang S et al (2018) Increasing concurrent drought and heat during the summer maize season in Huang-Huai-Hai Plain. *China International Journal of Climatology* 38(7):3177–3190
- Wang Z, He F, Fang W et al (2013) Assessment of physical vulnerability to agricultural drought in China. *Nat Hazards* 67(2):645–657
- Wei S, Liu J, Li T, Wang X, Peng A, Chen C (2020) Effect of high-temperature events when heading into the maturity period on summer maize (*Zea mays* L) yield in the Huang-Huai-Hai region China. *Atmosphere* 11(12):1291
- Wu D, Fang S, Li X, He D, Zhu Y, Yang Z, Xu J, Wu Y (2019) Spatial-temporal variation in irrigation water requirement for the winter wheat-summer maize rotation system since the 1980s on the North China Plain. *Agric Water Manag* 214:78–86
- Xue J, Zhang X, Zhang J et al (2021) Analysis of crop yield and water use efficiency of wheat-maize double cropping system under different irrigation systems based on APSIM model. *J Soil Water Conserv* 35(4):106–114
- Yang X, Leung LR, Zhao N, Zhao C, Qian Y, Hu K, Liu X, Chen B (2017) Contribution of urbanization to the increase of extreme heat events in an urban agglomeration in east China. *Geophys Res Lett* 44(13):6940–6950
- Yin Y, Zhang X, Lin D et al (2014) GEPIC-V-R model: A GIS-based tool for regional crop drought risk assessment. *Agric Water Manag* 144:107–119
- Zhang F, Chen Y, Zhang J et al (2019) Dynamic drought risk assessment for maize based on crop simulation model and multi-source drought indices. *J Clean Prod* 233:100–114
- Zhang JQ (2004) Risk assessment of drought disaster in the maize-growing region of Songliao plain. *China Agric Ecosyst Environ* 102:133–153
- Zhang Q, Zhang J, Wang C (2017) Risk assessment of drought disaster in typical area of corn cultivation in China. *Theor Appl Climatol* 128(3–4):533–540
- Zhang Q, Han J, Yang Z (2021) Hazard assessment of extreme heat during summer maize growing season in Haihe Plain, China. *International Journal of Climatology*. <https://doi.org/10.1002/joc.7099>
- Zhang T, Lin X, Sassenrath GF (2015) Current irrigation practices in the central United States reduce drought and extreme heat impacts for maize and soybean, but not for wheat. *Sci Total Environ* 508:331–342

Publisher's Note Springer Nature remains neutral with regard to jurisdictional claims in published maps and institutional affiliations.